OPTI-521 **Tutorial** **Chia-Ling Li** 2013/12/2

1. Introduction

Aspheric lenses have become synonymous with high-performance optics. They are used in an optical design to correct aperture dependent aberrations (spherical aberration), to correct field dependent aberrations (distortion and field curvature), to reduce weight, to make optical systems more compact, and in some cases to reduce cost. Fewer elements are needed, making systems smaller, lighter and shorter. For applications where weight is primary concern, space borne applications for example, aspheres are desired. This tutorial presents the design, fabrication, and testing of aspheric surfaces.

2. Design

2.1 Mathematical representation of aspherical surfaces

Aspheric lenses contain at least one optical surface of non-constant radius of curvature. The variability of radius is the primary differentiator from a spherical lens. The standard ISO 10110—Part 12 describes surface functions of second order with axial symmetry as

$$z = \frac{r^2/R}{1+\sqrt{1-(1+\kappa)(r^2/R^2)}} + \sum_{n=2}^{m} A_{2n} r^{2n} ,$$

where r is the radial coordinate, z is the sag, and R is the vertex radius of curvature. The conic constant κ is 0 for spheres, −1 for parabolas, <−1 for hyperbolas, between −1 and 0 for oblate ellipses and >0 for prolate ellipses [1]. The $A_{2n}r^{2n}$ terms are the even higher order aspheric terms. It is better to use even polynomials, not odd polynomials. The n starts with 2 since the n=1 term is redundant with base radius.

When optimizing an optical system that uses a higher order aspheric surface, a larger aperture than required for the clear aperture of the surface is necessary in design in order to control the polynomial inside the clear aperture and safely outside the margin of the clear aperture. Besides, more field points should be used in the optimization. On-axis, full field and 0.7 field points will sufficiently sample a system with all spherical surfaces, but systems with generalized aspheres should have seven to nine field positions in the model. Higher order aspheres improve performance in diamond turned optics and molded optics with little or no increase in cost or complexity. When designed correctly, higher order aspheres can improve the aspheric fit and reduce the departure and difficulty of the aspheric surface [2].

The traditional power series based aspheres present inherent complications when it comes to manufacturing and testing of these components. Other mathematical formulations such as Q-type polynomials (shown below) and Zernike polynomials have been employed over the years in an attempt to improve on the classic power-series method of modeling aspheric surfaces. These polynomials facilitate the determination of optimum placement of aspheric surfaces in an optical system. Their aspheric terms are orthogonal over a normalization radius, which makes each term unique and meaningful tolerancing of the terms possible [3].

$$z = \frac{r^2/R}{1+\sqrt{1-(r^2/R^2)}} + \frac{1}{\sqrt{1-(r^2/R^2)}}\left\{u^2(1-u^2)\sum_{n=0}^{m} a_n Q_n(u^2)\right\}$$

2.2 Aspheric shape design guide [4]

When designing an aspheric surface, some surface shapes should be avoided because they could increase the manufacture difficulty and the cost. If the optical designer understands what range of aspheric surfaces can be manufactured, they can constrain the aspheric surface during optimization. Many aspheric polishing machines have a minimum radius of curvature for concave surfaces because the polishing wheel or polishing tool has a physical radius that must be less than the radius of curvature of the work piece. Convex surfaces are not constrained by this limitation. A convex parabolic surface with a vertex radius of 15 mm can still be polished with a 35 mm radius polishing wheel. For this reason, if the surfaces being considered for aspherization are shorter than 35 mm vertex radius of curvature, aspherize a convex surface.

The steepness of the aspheric departure (the slope of the aspheric departure) often has a larger impact on manufacturing difficulty than the amplitude of the asphere or the steepness of the base radius. In general, any departure from the best fit sphere up to 1 or 2mm does not cause significant difficulty. The preferred and non-preferred surface shapes are listed in table 1.

Table 1. The preferred and non-preferred surface shapes

<table>
<tr><th>Preferred</th><th>Non-preferred</th></tr>
<tr><td>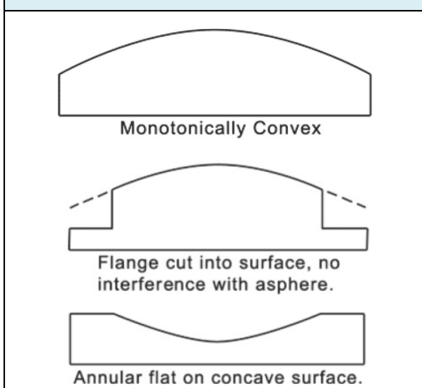
</td><td>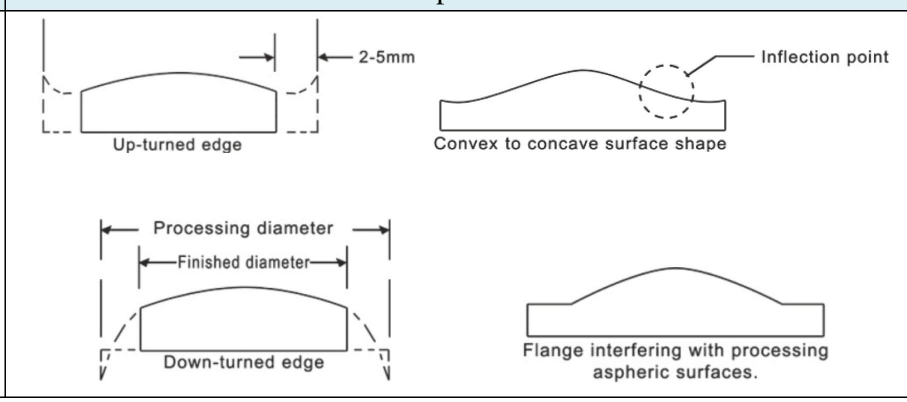
</td></tr>
</table>

2.3 Specifying tolerances for aspherical optical elements

Specifying an asphere begins with material selection and specification of diameter, thickness, cosmetics and clear aperture in the same way a spherical lens would be specified. The same style of tolerancing applies for these attributes as they would for a spherical lens. Table 2 lists the manufacturing tolerance from Optimax Systems, Inc.

Table 2. Manufacturing tolerance [5]

Attribute	Commercial	Precision	High Precision
Glass Material (n_d, v_d)	±0.001, ±0.8%	±0.0005, ±0.5%	Melt Data
Diameter (mm)	±0.00/-0.10	+0.000/-0.025	+0.000/-0.015
Center Thickness (mm)	±0.150	±0.050	±0.025
SAG (mm)	±0.050	±0.025	±0.015
Clear Aperture	80%	90%	90%
Radius (larger of two)	±0.2% or 5 fr	±0.1% or 3 fr	±0.05% or 1 fr
Irregularity - Interferometer (fringes)	2	0.5	0.2
Irregularity - Profilometer (microns)	±10	±1	±0.5
Wedge Lens (ETD, mm)	0.050	0.010	0.005
Wedge Prism (TIA, arc min)	±5	±1	±0.5
Bevels (face width @ 45°, mm)	<1.0	< 0.5	< 0.5
Scratch - DIG (MIL-PRF-13830B)	80 - 50	60 - 40	20 - 10
Surface Roughness (Å rms)	50	20	10
AR Coating (R_{Ave})	MgF_2 R < 1.5%	BBAR R < 0.5%	V-coat R<0.2%

Figure 1 shows a drawing of an aspherical lens element. The design equation with its constants and coefficients is given in the field of the drawing. The coordinate axes are indicated in the drawing. An abbreviated table with some function values is shown for information. It is especially useful to check for the correct signs of the constants and the coefficients. The indications are arranged in tabular form, according to ISO 10110-10. This prevents the drawing from being overloaded. The indications refer to the left and right surface and to the material data, given at the center of the table. The permissible form deviations are specified following the error code 3/, and tolerances for the position deviations of the surfaces follow the error code 4/. The form tolerances of the asphere are given according to ISO 10110-5 as 3/4(0.8/0.4), which means a sag error of 4 fringes (@ λ = 546 nm), a total irregularity of 0.8 fringes, and a rotational symmetric irregularity of 0.4 fringes are permissible. Because the axis of the asphere is the datum axis, no tolerance for the tilt angle is specified following error code 4/. The runout of the outer cylinder is limited to ≤0.005, according to ISO 1101. For the slope tolerance, no error code exists. Therefore, the tolerance is indicated as a text note in the field of the drawing, according to ISO 10110-12.

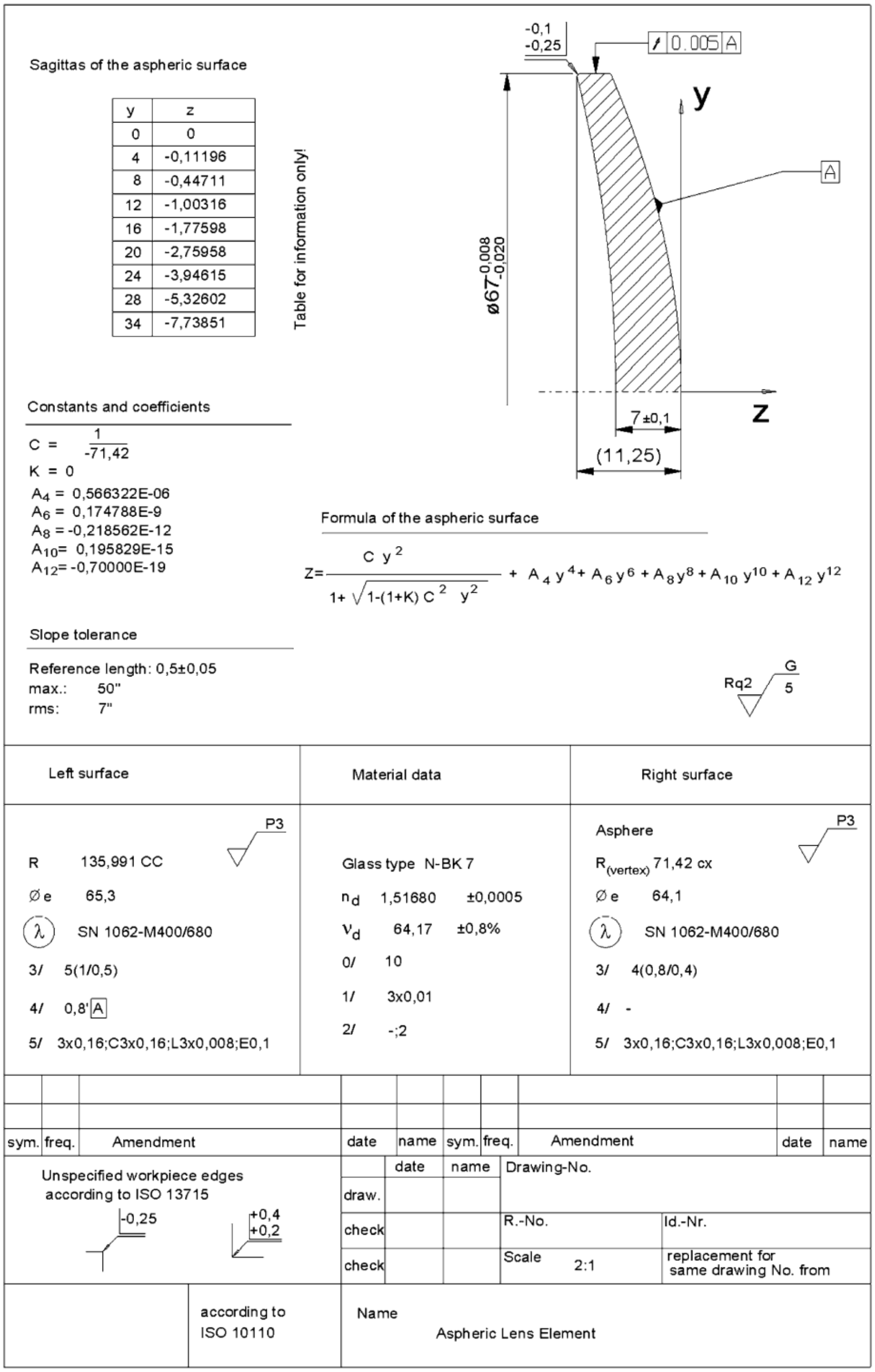

Figure 1. Drawing of an aspherical lens element according to ISO 10110 [1].

3. Fabrication

In general, all glasses can be used for aspherical lenses. For standard glasses, the manufacturing is performed by computerized numerical control (CNC) grinding and magnetorheological finishing

(MRF) polishing. The contour is controlled by tactile and holographical measurements and finished in several optimization loops per lens. This process can only deliver small lot sizes at high costs, typical for industrial optics. Aspherical glass lenses can also be produced by precision molding.

Aspherical polymer lenses can be produced very cost-effectively via injection-molding processes. In specific cases one can use diamond turning, but mainly for fast prototyping. The weak points of polymers are the strong temperature dependence of their optical properties, insufficient long-term stability, sensitivity to radiation impact and humidity, outgassing, and transmission loss in the blue and UV part of the spectrum. Also, the variation of the refractive index from production lot to lot has to be controlled. Although the refractive index of glass can be fine-tuned and controlled by an annealing process, this is not possible for polymers. Typically used polymers are PMMA, polystyrene (PS), polycarbonates (PC), cyclo-olefin polymers (COC, e.g., Zeonex®), CR39, and the resin MR-8. Because the optical position of these polymers is not controllable with high accuracy during production, lens systems often have to be corrected during assembly (melt-dependent production).

The production of aspherical lenses from crystals requires CNC machining or diamond turning. Therefore, high material costs, together with high machining costs, lead to expensive lenses, affordable only in industrial or military instruments. Figure 2 shows the manufacturing cost of different materials.

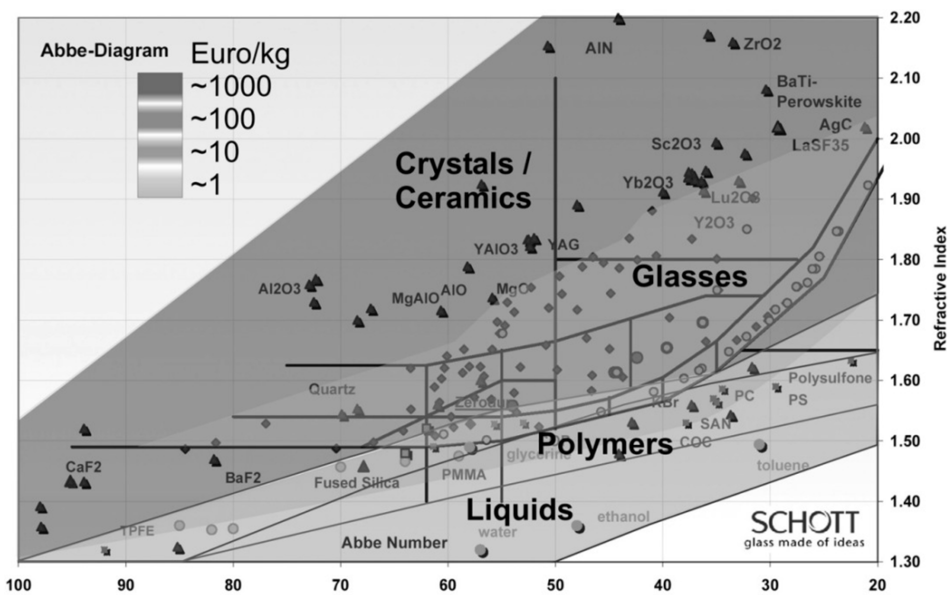

Figure 2. Principal price sectors of materials [1].

Figures 3 and 4 give an overview of the different types of processing available. The classical fabrication is listed in more detail in Fig. 4. The characteristic features of each process step are discussed in Table 3. Due to the nonperfect polishing step or based on the required final surface specification, the aspheric element has to pass a third process step, local correction. Residual surface deviations from the nominal shape have to be removed by this process step. The methods of local correction include computer controlled polishing (CCP), fluid jet polishing, magnetorheological finishing (MRF), and ion beam figuring (IBF).

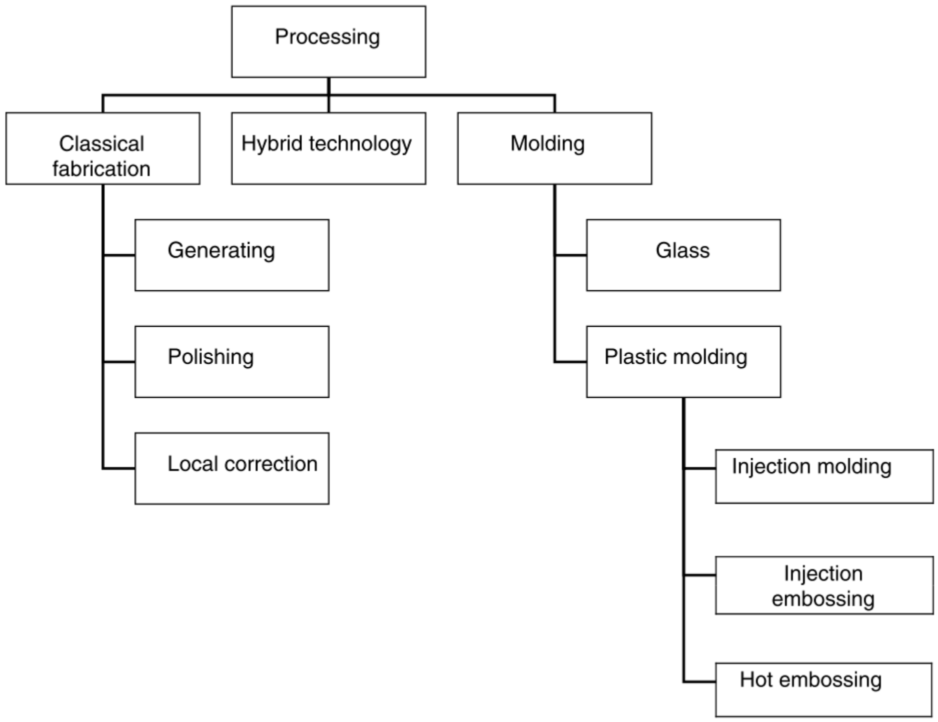

Figure 3. Overview of different kinds of process technologies [1].

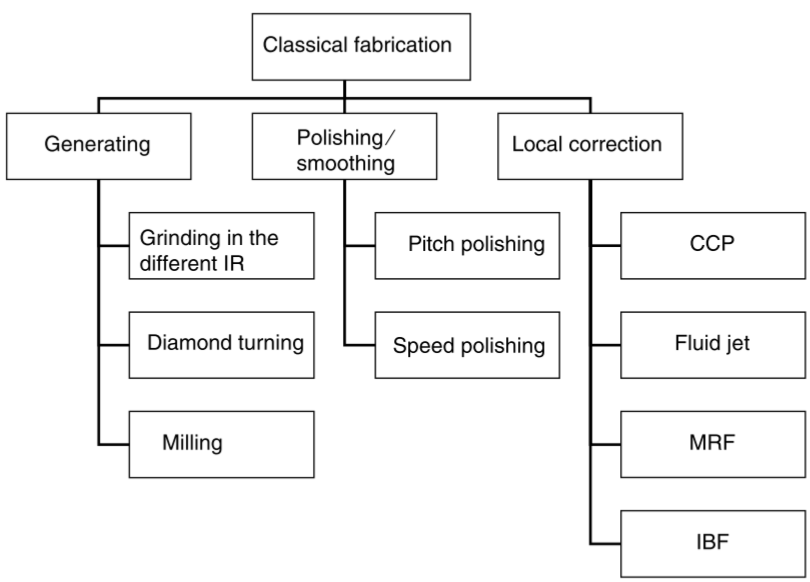

Figure 4. Detailed structure of classical optics fabrication [1].

Table 3. Overview specifications and characteristics of the different processes (typical values in production) [1].

Process	Batch size	Size (mm)	Shape deviation (nm) PV	Surface roughness (nm) rms	Advantages	Limits	Main cost driver
Grinding	$<10^4$	2–400	1000	50–1000	Fast generating process	Subsurface damage	Size, accuracy
Diamond turning	$<10^3$	2–400	100	5–20	No subsurface damage, for IR sufficient roughness	Surface roughness	Size, accuracy
Speed/pitch polishing	$<10^4$	10–300	300	0.2–0.5	Very low surface roughness, fast polishing process	Correction of local surface deviations	Size
CCP	$<10^3$	5–8000	30	0.5	30 years experience	Tool wear, edge roll-off	Size
MRF	$<10^3$	5–500	10	0.3	No edge roll-off, no tool wear, low damaged surface layer	Center artefact for r–φ tool path	Size, fluid
Fluid jet	$<10^3$	5–240	30	0.5	No edge roll-off	Stability of foot print	Size
IBF	$<10^3$		5	0.2	No edge roll-off	Low removal rate	Vacuum
Precise glass pressing	10^4 to $>10^6$	0.5–35	1–5	2	High volume	Size, accuracy	Cycle time, accuracy
Injection molding	10^4 to $>10^6$	0.5–200	1–10	5	High volume, complicated shapes possible	Birefringence, micro structures	Accuracy
Injection/hot embossing	10^4 to $>10^6$	0.5–200	1–10	5	Low birefringence, optics including mounting	Thickness	Cycle time accuracy

CCP: computer controlled polishing; MRF: magnetorheological finishing; IBF: ion beam figuring.

The measurement of aspheres in the production process is of essential importance for achieving the final desired surface. Since the production sequence is iterative, several steps must be taken between surface shaping and measurement before the required accuracy level is achieved. Figure 5 shows an example of the general fabrication procedure.

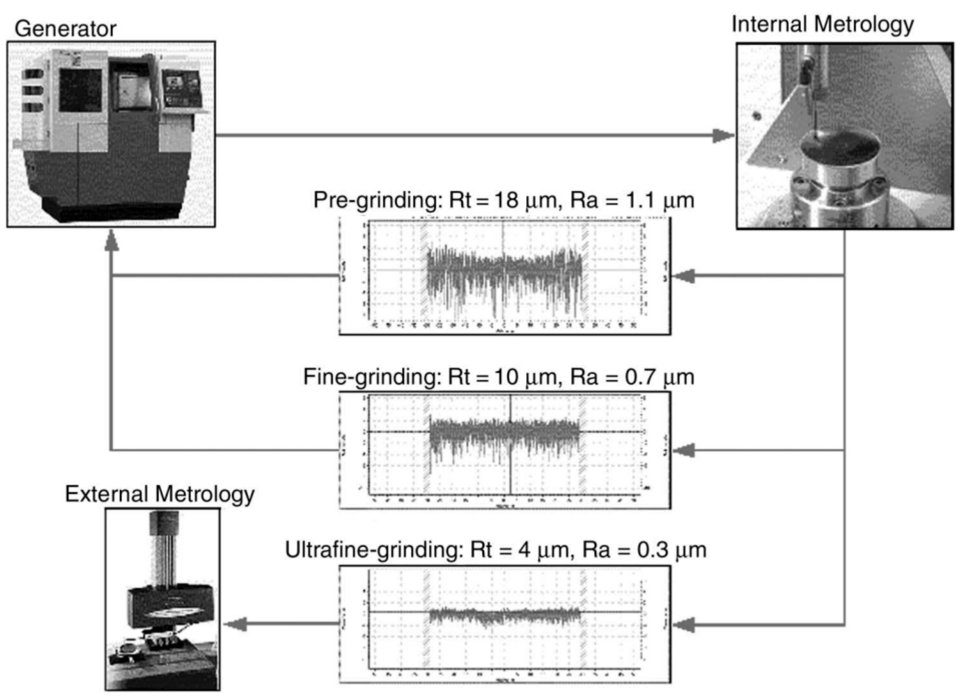

Figure 5. Integration of grinding process and metrology [1].

4. Testing

In recent years, the production of these elements has seen an overwhelming increase, in part due to the development of new fabrication technologies such as computer-controlled polishing, magnetorheological finishing and ion beam figuring. These techniques allow the deterministic polishing of precise surfaces in less time than was previously possible. As the fabrication of extremely accurate surfaces has proliferated, so too has the demand for high-precision measurement. After all, one cannot produce surfaces better than it is possible to measure. The three main metrology options are profilometry, interferometry in reflection, and interferometry in transmission.

4.1 Profilometry [5]

This is the most commonly used metrology option for aspheric forms. The device measures height of the surface as a function of movement along one axis, producing a 2-D table of data. Using information about the ideal form and how the profilometer is set up, the data is analyzed, showing error from theoretical form with setup related tilt removed. Measurement certainty here is ~0.1 μm at best, and it decreases for extremely steep or extremely flat surfaces.

4.2 Interferometry in reflection

Reflective interferometry for aspheres works in the same manner as spheres or flats, except the null target is unique to the specific desired ideal aspheric form. There are four reflective techniques here, on-axis measurement for mildest forms, subaperture stitching for more complex forms, holographic testing for the most complex forms, and flexible measurement techniques.

4.2.1 On-axis measurement [5]

For some cases the asphericity is mild enough where an interferometer can see through the aberrations present. On-axis testing with a Zernike based aberration subtraction is sufficient. This process is typically reserved for aspheres of less than < 10μm of aspheric departure and < 150mm of diameter. Allowable departure is proportional to diameter.

4.2.2 Subaperture stitching [5]

More departure can be handled by stitching interferograms together. Using QED's Subaperture Stitching Interferometer (SSI) or Zygo's VeriFire AT mild aspheric forms can be formed using conventional transmission spheres. While moving the part until the local curvature becomes manageable, several (ranging from ~5 to ~100) overlapping measurements are made. A full aperture representation of the deviation of the aspheric surface is formed by stitching the measurements together. Broadly speaking the present limit is < 50μm of aspheric departure and < 200mm of diameter. Allowable departure is proportional to diameter.

4.2.3 Holographic testing [5-8]

Interferometric testing is still possible for larger departures using a holographic null. Figure 6 shows the computer generated hologram (CGH), and Fig.7 shows the setup of the CGH-based null testing. Each asphere requires its own null, each costing about $10 – 15K and taking about 10 – 15 weeks to get. Measurement certainty is about λ/8 at HeNe here, as setup induced errors are difficult to identify and eliminate. While less sensitive, the same issues of rate of change and location of departure still apply. Lenses that may be measured interferometrically can be specified in the same manner as any spherical surface, with a linear tolerance on the vertex radius and the irregularity as the deviation from aspheric form.

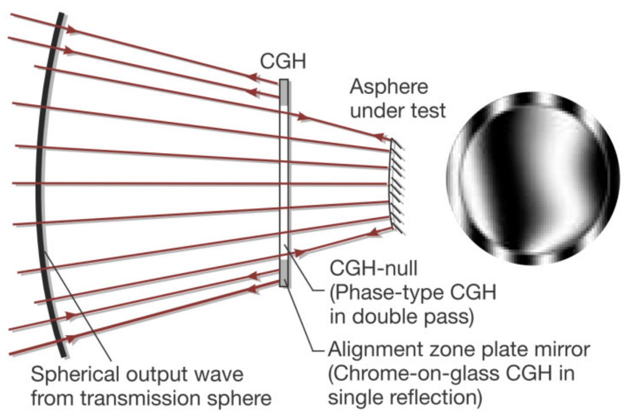

Figure 6. (Left) The alignment ring is a diffractive mirror that retroreflects the spherical wave coming from the transmission sphere when the CGH is placed in the correct position. (Right) Simulated interferogram showing some misalignment (external ring-shaped interferogram) [7].

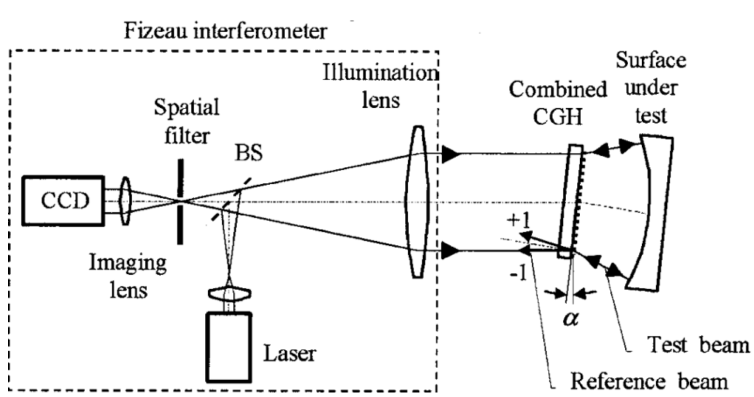

Figure 7. Layout of a null CGH test of an aspherical surface, using one single CGH working in a collimated interferometer beam without reference flat [8].

4.2.4 Flexible measurement techniques [7]

The increasing availability of CGH has made diffractive null optics an economic alternative to refractive and reflective null optics. Nevertheless, testing with individual null optics is not an economic solution for the production of small-series or prototype aspheres. Also, the production times (design and fabrication itself) for the null corrector might become prohibitive. Current research efforts are oriented toward developing alternative techniques for the rapid, flexible and precise characterization of aspheric surfaces.

Recently, researchers have proposed an approach (Fig. 8) that targets the boundary condition of process-integrated aspheric testing. It avoids all mechanical movements of the surface under test, but works instead with a non-standard illumination. As opposed to a standard interferometer, where only one wavefront impinges onto the surface under test, this new type of interferometer uses many wavefronts simultaneously; they are generated using an array of coherent point sources.

This strategy allows for the parallel measurement of aspheric surfaces in a very short time, even for strong aspheres with deviations from the best-fit sphere of several hundred microns. Each source generates a defined test area on the surface of the test element where no subsampling or vignetting takes place. The system is designed such that the measurement areas generated by the whole source array cover the whole surface of the asphere.

Leaving the null-test configuration enables a wide dynamic range in the asphericities to be measured but also implies that the interferometer must be fully characterized in order to separate the phase contributions of the interferometer itself and the wavefront being measured. Thus, special calibration and measurement procedures were developed to cope with the effects of the so-called retrace aberrations introduced by the non-null test configuration.

The interferometer is designed to achieve an accuracy of $\lambda/30$ with sag deviations from the best-fit asphere of up to 1,000 µm; it has shown a measurement time of less than 40s. Although the system has been developed for the testing of aspheres, it is capable of measuring mild free-form surfaces with deviations of the surface normals from the best-fit sphere of up to 5°.

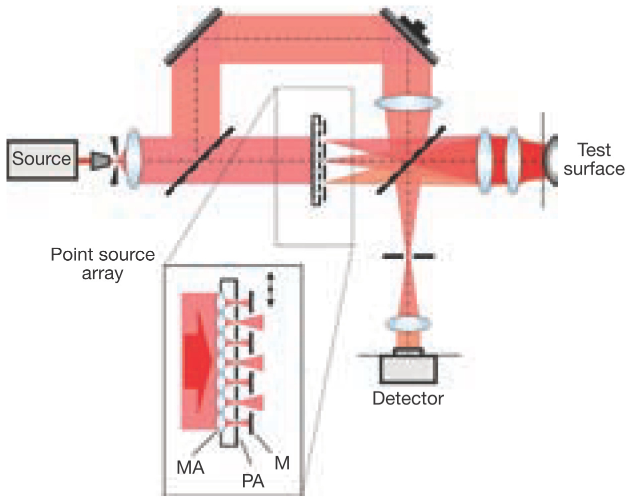

Figure 8. Interferometer with multiple test beams. A point source array generates several tilted wavefronts that reach the test surface under different angles. MA=microlens array; PA=point source array; M=source selection mask [7].

4.3 Interferometry in transmission [5]

For aspheric lenses, there are some specific cases where testing in transmission as opposed to reflection offers a simpler solution. It is possible with one simple null assist optic or even none at all an asphere may be tested, saving time and money over reflectance testing. The test measures literal transmission wavefront error (TWE), looking at the sum of all errors. It sums up the contributions from errors in centration, form and material. This sum is targeted and corrected. This is an extreme special case.

Table 4 lists the comparisons of the asphere metrologies.

Table 4. Asphere metrology [5]

Method	Cost of Test Setup[1]	Setup Time[2]	Test Time[3]	Tolerance Limit	Max. Departure	Comments
Surface Contact Measurement						
CMM	Low	Minutes	~10 min	± 5μm	mm	No required symmetry; requires datum & fixturing
Profilometry	Low	Minutes	~5 min	± 0.5μm	<25 mm	Most common method; only provides 2D data
Surface Testing in Reflection						
Spherical Wavefronts	Low	Minutes	~10 min	0.1 Fringes	<10 μm	Zernike subtraction; fringe density limited
CGH	High	Months	~20 min	0.25 Fringes	mm	No required symmetry; part specific
Spherical Null Reflection	High	Weeks	~10 min	0.1 Fringes	100 μm	Part specific
Parabola/Ellipse	Average	Hours	~30 min	0.1 Fringes	mm	$-1 \leq k > 0$
Subaperture Stitching	Average	Minutes	~30 min	0.1 Fringes	<650 μm	Absolute test
Annular Ring Stitching	Average	Minutes	~15 min	0.1 Fringes	<800 μm	Discontinuous at sagittal zero curvature
Lens Testing in Transmission						
TWE	Average	Hours	~10 min	0.1 Fringes	<50 μm	Must be well-behaved aspheric lens
CGH	High	Months	~20 min	0.25 Fringes	mm	No required symmetry; part specific
Spherical Null TWE	High	Weeks	~10 min	0.1 Fringes	~100 μm	Part specific

5. Conclusions

Aspheres, which are designed to null out a unique set of aberrations, are specified using the aspheric equation. The manufacturing process is a function of the best fit sphere and the departure. A suitable manufacturing method is chosen according to the lens materials and the required accuracy. There are many metrology options, with selection driven by departure, form error and cost objectives.

6. References

1. B. Braunecker, R. Hentschel, and H.J. Tiziani, “Advanced Optics Using Aspherical Elements”, SPIE ebook, 2008.
2. J. Kumler, “Designing and Specifying Aspheres for Manufacturability”, Jenoptik Optical Systems, Inc.
3. Synopsys, Inc., “Asphere Design in CODE V” datasheet.
4. Kreischer Optics, Ltd., “Aspheric Design Guide”.
5. http://www.optimaxsi.com/capabilities/aspheres/
6. J.C. Wyant, “Interferometric Testing of Aspheric Surfaces”, SPIE Interferometric Metrology, Vol. 816, pp.19-39, 1987.
7. C. Pruss, E. Garbusi and W. Osten, “Testing Aspheres”, Optics & Photonics News, pp. 25-29, Apr. 2008.
8. J.M. Asfour and A.G. Poleshchuk, “Asphere testing with a Fizeau interferometer based on a combined computer-generated hologram”, J. Opt. Soc. Am. A, Vol. 23(1), pp. 172-178, 2006.